ISSN 1027-5495. Functional Materials, 33, No.1 (2026), p. 70-82
doi:http://dx.doi.org/10.15407/fm33.01.70 © 2026 — STC "Institute for Single Crystals"
This is an open access article under the CC BY-NC-ND license (http://creativecommons.org/licenses/by-nc-nd/4.0/).

Adsorption and corrosion prevention efficacy of *Hyppomarathrum libanotis* butanolic extract on API 5L Gr-B steel in acid environment

Kaouthar Soudani[1], Merzoug Benhmed[2], Abdelkader Hafdallah[3*], Hocine Laouar[4], Abdelkrim Gouasmia[1]

[1] Laboratory of Organic Materials and Heterochemistry, Echahid Cheikh Larbi Tebessi University, 12002, Tebessa – Algeria
[2] Laboratory of Bioactive Molecules and Applications, Echahid Cheikh Larbi Tebessi University, Tebessa – Algeria
[3]Applied and Theoretical Physics Laboratory, Department of Materials Sciences, Echahid Cheikh Larbi Tebessi University-Tebessa, Constantine Road, Tebessa 12002, Algeria
[4]Laboratory for the valorisation of natural biological resources Ferhat Abbas University, Setif, Algeria
[*]abdelkader.hafdallah@univ-tebessa.dz

Received April 9, 2025, approved September 24, 2025

Environmental sustainability is a serious problem, which needs to be overcome for practical application. Therefore, our goal is to develop the butanolic extract of the plant *Hyppomarathrum Libanotis* (EBHL), belonging to the Apiaceae family, as an API 5L Gr-B carbon metal deterioration inhibitor in 1M HCl solution. To test the efficacy of inhibition, the effects of solution concentration, immersion time, and temperature on the deterioration processes of API 5L Gr-B metal in 1 M HCl medium in the presence of an inhibitor were studied. The study included mass loss analysis, electrochemical impedance spectroscopy, and potentiodynamic polarization. The obtained tests showed that increasing the concentration improves the output of EBHL inhibition and achieves a value of 82 % at 700 ppm. The temperature rise contributed to a major drop in the production of inhibitions. Potentiodynamic polarization tests indicate the role of the extract as a dual-action inhibitor. In the Langmuir isotherm model, the main influence is on the anodic region, and as a result, a retention process occurs. Based on the above results, thermodynamic and activation parameters were established. Furthermore, deep structural and chemical analysis was also performed. X-ray photoelectron spectrometry and scanning electron microscopy were utilized for the study. The results indicate the formation of a protective coating on the carbon steel sheet..

Keywords: Acid, inhibitor, steel, polarization, impedance, SEM, XPS

Адсорбційна та антикорозійна ефективність бутанольного екстракту Hyppomarathrum libanotis на сталі API 5L Gr-B у кислотному середовищі. *Kaouthar Soudani, Merzoug Benhmed, Abdelkader Hafdallah, Hocine Laouar, Abdelkrim Gouasmia*

Екологічна стійкість є серйозною проблемою, яку треба подолати для практичного застосування. Тому наша мета - розробити бутанальний екстракт рослини Hyppomarathrum Libanotis (EBHL), що належить до сімейства Apiaceae, API 5L Gr-B як інгібітор руйнування металу в 1M HCl. Для перевірки ефективності інгібування були проведені дослідження впливу концентрації розчину, періоду занурення та температури на процеси руйнування

металу API 5L Gr-B в середовищі 1M HCl у присутності інгібітору. Дослідження включало аналіз втрати маси, електрохімічну імпедансну спектроскопію та потенціодинамічну поляризацію. Отримані тести показали, що збільшення концентрації покращує вихід інгібування EBHL і досягає значення 82% при 700 ppm. Підвищення температури сприяло значному зниженню інгібування. Потенціодинамічні поляризаційні тести вказують на роль екстракту як дворежимного інгібітора. Насамперед вплив на анодну область і процес утримання відбувається в моделі ізотерми Ленгмюра. На підставі наведених вище результатів встановлено параметри термодинаміки та активації. Крім того, було також проведено глибокий структурний та хімічний аналіз зразків. Для дослідження використовувалися рентгенівська фотоелектронна спектрометрія та скануюча електронна мікроскопія. Результати вказують на захисне покриття, що утворюється на листі вуглецевої сталі.

1. Introduction

It is a natural phenomenon that metal corrosion changes, degrades and transforms the chemical and physical properties of metals. This process is recognized as a serious problem in industrial sectors and is the subject of extensive scientific investigation. During certain tasks, such as cleaning, tartrate extraction, unsealing, or transportation, the metal may come into intense contact with the hydrochloric acid, resulting in significant corrosion. The organic inhibitors attach to the metal surface through the arrangement of π-electrons and heteroatoms such as P, N, O, and S. There are two types of adsorption: chemisorption and physisorption. The use of inhibitors has become one of the most effective approaches. As a result of extensive research and study of optimal strategies, superior solutions for protecting metals from corrosion have been developed. Despite the good inhibitory efficacy of synthetic compounds, the utilization of these compounds is constrained by their elevated expense, non-biodegradable nature, and harmful impacts on both humans and the environment. To overcome these limitations, recent research has increasingly focused on corrosion-inhibiting properties and the development of stable, non-toxic organic molecules. To protect the environment, it is necessary to use natural, biodegradable and affordable products. The genus *Hyppomarathrum libanotis* is a member of the Apiaceae family, which includes sunflowers. Simple extraction methods are typically used to create plant extracts, which exhibit good inhibitory properties in acidic environment. This study examined the impact of *Hyppomarathrum libanotis* butanolic extract on adsorption and the inhibition of corrosion. The analysis was performed through evaluation of weight loss; potentiodynamic polarization, and electrochemical impedance methods were used. Using X-ray photoelectron spectrometry and the SEM, morphological and chemical surface investigations were conducted to supplement this work.

2. Experimental

Flavonoids, tannins, and phenols were identified as components of the butanolic extract of *Hippomarathrum libanotis* by means of phytochemical evaluation.

Table 1 summarizes the outcomes of this examination. **[**1**]**

The total content of phenolic compounds and flavonoids in the butanol fraction was determined using the Folin-Ciocalteu reagent, and the measurement results are presented as quercetin equivalents (QE) and gallic acid equivalents (GAE), respectively. The results of these analyses indicate that the butanolic extract of *Hippomarathrum Libanotis* is rich in polyphenols, with a content of 371.2549 ± 12.88871 mg GAE/g (sample). Furthermore, the flavonoid and tannin contents were quantified at 64.2221 ± 4.522274 mg QE/g and 0.5211 ± 0.0081, respectively.

2.1. Preparation of Solutions

The corrosive solution is an acidic solution (1 M HCl), prepared by adding varying amounts of butanolic extract from the *Hippomarathrum Libanotis* to concentrated hydrochloric acid (37%) diluted with distilled water.

2.2. Specimen Preparation

For testing and measurements, limited steel confirmation samples with an area of 10.7 cm^2 containing Mn (1.15%), C (0.26%), P (0.05%) and S (0.04%) relative to the main Fe are used. Before each experiment, polishing was carried out with abrasive paper with a decreasing grain

Table 1. Findings of the phytochemical evaluation of *Hippomarathrum Libanotis* plant extract.

TPC (µg GAE/mg)	371.2549 ± 12.88871
TFC (µg GAE/mg)	64.2221 ± 4.522274
Tanin	0.5211 ± 0.0081

GAE: gallic acid, QE: quercetin, TPC: Total Phenols, TFC: Total flavonoids.

size from 150 to 2000, after which the surface was washed with distilled water and degreased with acetone.

2.3. Weight Loss Measurement

Accurate calculation of the overall corrosion coefficient using the bayonet gravimetric process is one of the first methods to study the interaction of inhibitor and metal. The corrosion rate of carbon steel (W_{corr}) is measured by gravimetric methods under both inhibitor and non-inhibitor conditions at different concentrations after 7 hours of exposure to the corrosive medium. The corrosion rate and inhibition efficiency of EBHL are evaluated using the relations (I.1) and (I.2), respectively:

, (I.1)

. (I.2)

Here $\Delta m = (m_1 - m_2)$ is the difference between the initial mass m_1 and the final mass m_2 after exposure t; S is the portion of the metal exposed to the solution. The corrosion rate was obtained by averaging the value of three tests carried out under the same conditions for each concentration. V_{corr} and V°_{corr} represent the corrosion degree without and in the presence of inhibitors, respectively **[2].**

2.4. Electrochemical measurements

Electrochemical analyses, as well as potentiodynamic polarization, equilibrium potential determination and impedance spectroscopy were carried out using a potentiostat controlled by Volta lab-PGZ 301 software. Low-carbon steel was used as the functional electrode, and a platinum rod was used as the counter electrode. At the same time, Ag/AgCl fully impregnated with calomel was used as the base electrode. In the electrochemical method, the processes were carried out after 1 hour of exposure in the solution to obtain a reliable open circuit potential. The measurements were carried out in the voltage range from -250 to +250 mV at a rate of 1 $mV \cdot s^{-1}$ compared to the possible open circuit potential. For efficiency inhibition calculation, Eq. (II. 1) was used **[3]:**

. (II. 1)

Here i_{corr} and i°_{corr} are intensities of the deterioration current with and without inhibitor, respectively. The EIs were recorded in the range from 100 kHz to 0.01 Hz with an amplitude of 10 mV.

Using EC- Lab software, the HIA data and suit curves were simulated. Equation (II. 2) was used to determine the inhibition potency from polarization resistance measurements **[4]**.

$$IE(\%) = \frac{R_p^{\circ} - R_p}{R_p^{\circ}} \times 100 \,. \qquad \text{(II. 2)}$$

Here R°_p and R_p are the resistance to polarization of the metal with the inhibitor excluded and included, respectively.

2.5. Surface morphology and chemistry studies

To observe the surface topography, scanning electron microscopy (SEM) was used with on a JEOL JSM 7500F instrument at an accelerating voltage of 15 kV. X-ray photoelectron spectroscopy (XPS) analysis was performed on a Kratos Axis Ultra instrument using Al-*K*α radiation (1486.6 eV) for surface analysis. Detailed profiles were recorded at an operating energy of 20 eV, achieving a power resolution of 0.9 eV. Binding energies were corrected for charge shifts, using the C 1s line at 284.4 eV as the reference. The interval was corrected by subtracting the Shirley background signal, and symmetric Gaussian functions were used to fit the peaks.

3. Results and discussion

3. 1. Weight loss

After seven hours of exposure of API 5L Gr-B metal samples to 1.0 M HCl solution in the absence/presence of butanol extract of the plant *Hippomarathrum libanotis* (EBHL), the corrosion rate, the recovery rate and the inhibitor efficiency of EBHL were analyzed in the temperature range from 293 K to 323 K. A detailed review of the results presented in Table 2 indicates a significant reduction in the corrosion rate of CR, accompanied by an increase in inhibition efficiency with higher EBHL concentrations. At 700 $mg \cdot L^{-1}$, we suggest that the amount of assimilated inhibitor particles increases and covers the active sites on the outer layer of API 5L Gr-B steel [5, 6]. Figure 1 shows that as the solution temperature elevates from 293 to 323 K, the corrosion rate rises, and the inhibitor efficiency (IE) slightly decreases. This effect is explained by the increased detachment of inhibitor molecules from the metal surface or the weakening of the adsorption mechanism, which indicates the role of physical adsorption [7, 8].

Table 2. The influence of EBHL concentration on inhibitory efficacy at different temperatures (293-323) K

C (mg. L^{-1})	293 K			300 K			313 K			323 K		
	CR (mg cm^{-2} h^{-1})	Θ	IEw(%)	CR (mg cm^{-2} h^{-1})	θ	IEw(%)	CR (mg cm^{-2} h^{-1})	θ	IEw(%)	CR (mg cm^{-2} h^{-1})	Θ	IEw(%)
0	0.2102	-	-	0.2817	-	-	0.3663	-	-	0.4300	-	-
100	0.1400	0.3341	33.41	0.1923	0.3171	31.71	0.2860	0.2193	21.93	0.3575	0.1686	16.86
300	0.0780	0.6291	62.91	0.1082	0.6157	61.57	0.2022	0.4480	44.80	0.2667	0.3798	37.98
400	0.0633	0.6987	69.87	0.0916	0.6749	67.49	0.1772	0.5160	51.60	0.2384	0.4455	44.55
500	0.0514	0.7556	75.56	0.0821	0.7084	70.84	0.1566	0.5725	57.25	0.2169	0.4955	49.55
600	0.0473	0.7750	77.50	0.0727	0.7417	74.17	0.1445	0.6054	60.54	0.2024	0.5293	52.93
700	0.0428	0.7965	79.65	0.0688	0.7559	75.59	0.1334	0.6358	63.58	0.1892	0.5600	56.00

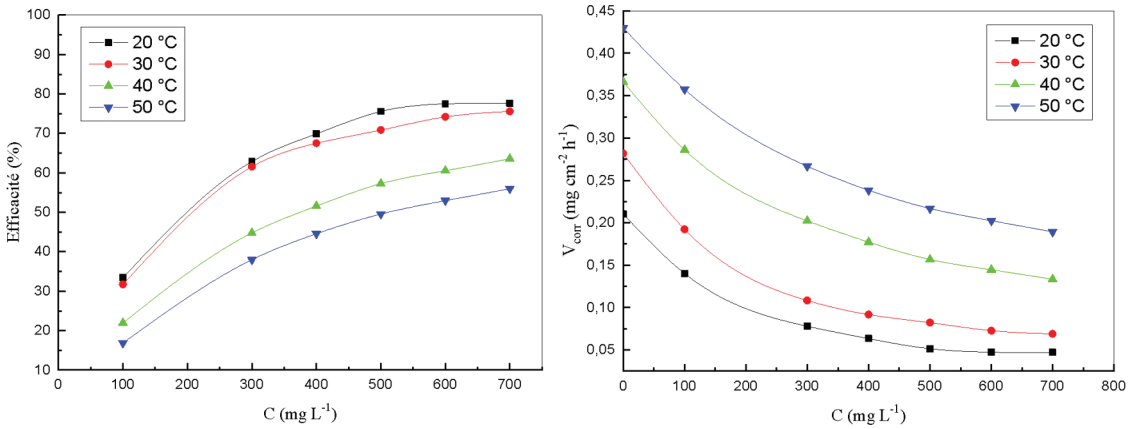

Fig 1. Evolution of corrosion rate and inhibition efficiency depending on EBHL concentration in 1M HCl solution at various heat degrees

3.2 Model of EBHL adsorption isotherms

Studying adsorption isotherms provides information on the interaction of the metal with the inhibitor. Several authors use the Langmuir, Temkin and Freundlich isotherms, and their ability to describe the binding of EBHL on API 5L Gr-B metal was compared based on the R^2 coefficient regression and slope values. At all temperatures, the regression values of the coefficients (R^2) were close to unity (according to the table), which confirms that the binding of EBHL on the outer layer of API 5L Gr-B follows the Langmuir isothermal model [9].

Figure 2 shows the Langmuir isotherm, and the recovery rate (C/θ) was assessed in relation to EBHL concentration at several temperatures. The K_{ads} value is determined by the intersection point of the linear segments, as shown in Table 3. The decrease in K_{ads} values with increasing temperature is associated with desorption of EBHL molecules from the surface of API 5L Gr-B [10]. The Langmuir adsorption isotherm corresponds to the recovery rate, which is related to the concentration of the extract by the following equation (III. 1):

$$\textbf{Langmuir}: \frac{C}{\theta} = \frac{1}{K} + C \qquad \text{(III. 1)}$$

In this context, C denotes the amount of inhibitor present, and θ indicates the extent of surface saturation at different inhibitor levels in 1 M HCl, and K_{ads} is the adsorption equilibrium constant.

Table 3. Regression coefficients

Model of isotherms	Temperature (K)			
	293	300	313	323
Langmuir	0.999	0.998	0.999	0.999
Temkin	0.997	0.996	0.9665	0.998
Freundlich	0.996	0.997	0.9664	0.996

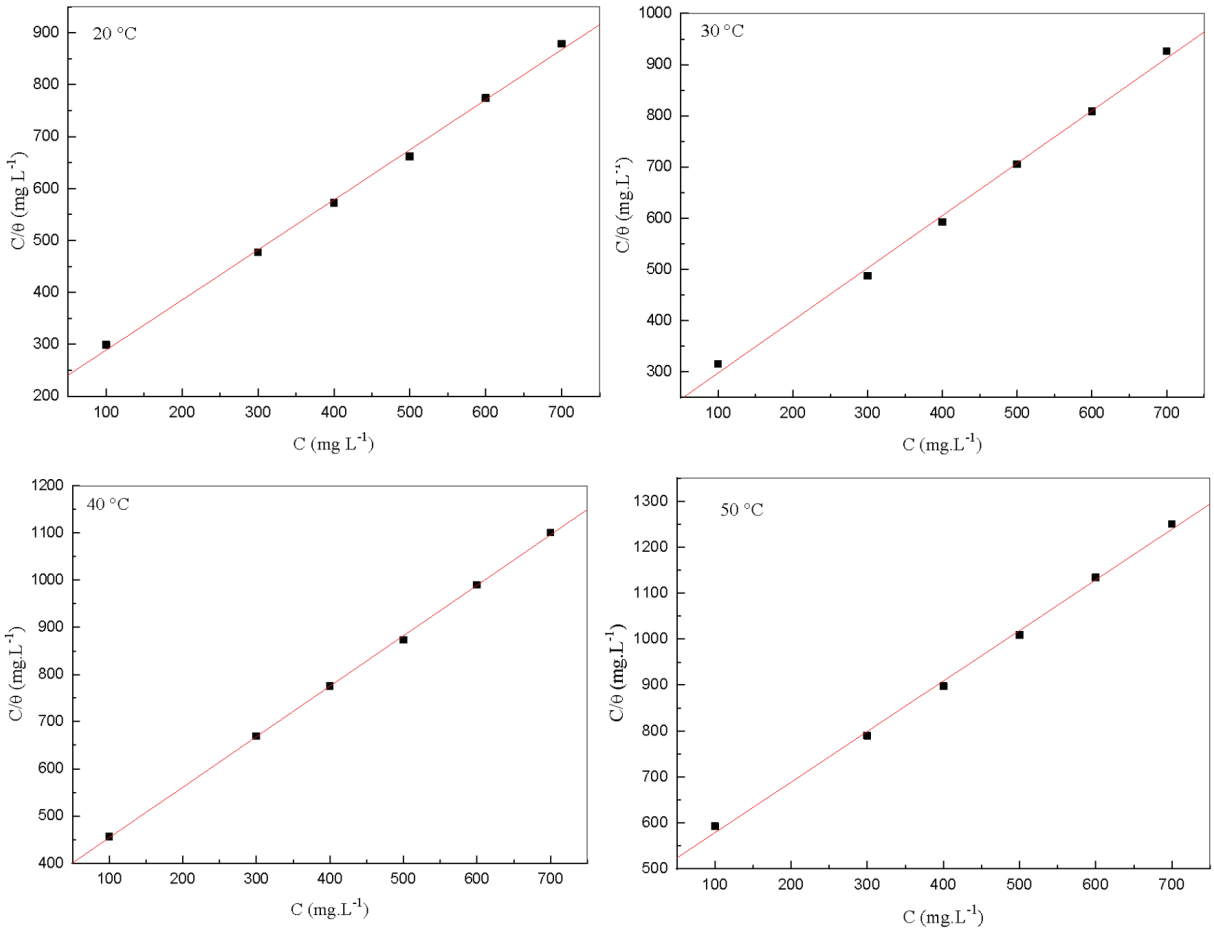

Fig. 2. Langmuir retention isotherm of EBHL on the metal superficies API 5LGr-B in 1M HCl solution in various temperature ranges

3. 3. Electrochemical measurements

3. 3. 1. Open-circuit potential control

Figure 3 shows the changes in the open circuit potential (E_{ocp}) for CS in a 1.0 M HCl solution in the absence/presence of EBHL at 298 K.

The working electrode is placed in the solution for 60 minutes, both with and without the addition of EBHL, to assess the current intensity of the solution and establish a steady state. This provides a fairly reliable basis for visualizing polarization curves and electrochemical impedance diagrams (corrosion potentials). This can be demonstrated from the corrosion free potential, which started at -510 mV/ECS and increased to slightly fluctuating values around -494 mV. This leads to a rapid dissolution, accompanied by the formation of a protective coating on the metal surface.

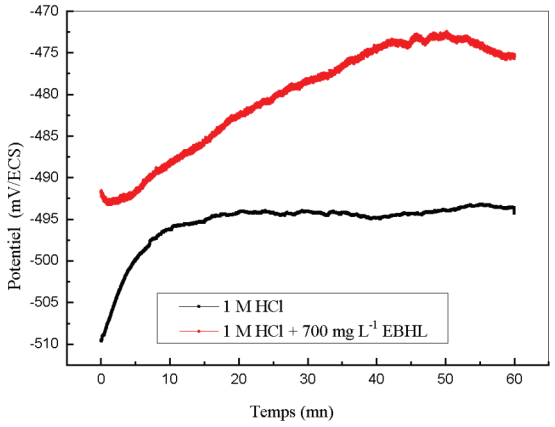

Fig 3. Evolution of abandonment potential in the 1 M HCl solution in the absence/presence of EBHL

3.3.2. Potentiodynamic Polarization Studies

Figure 4 shows the cathodic and anodic polarization curves of API 5L Gr-B metal in a 1M HCl medium, both without and with vari-

ous concentrations of EBHL, after a one-hour of exposure at room temperature. The electrochemical parameter values derived from these polarization curves are summarized: corrosion current density (I_{corr}), corrosion potential (E_{corr}), recovery rate, as well as corrosion inhibiting efficiency η_p(%). According to the polarization curves, after the addition of EBHL, a decrease in the current density in the region of the cathodic and anodic Tafel constants ($ß_a$ and $ß_c$) was observed. Both the anode and cathode curves exhibited fluctuations at lower current density levels **[**11**]**. The variations in E_{corr} values indicate the generation of a film on the surface of the metal **[**12**]**. The obtained data allowed us to understand the inhibition mechanism, which is based on blocking active regions on the iron surface [13]. Therefore, it can be concluded that this compound is a mixed-type inhibitor. On the other hand, it is noted that the inhibitory effectiveness diminishes at elevated temperatures, which may be a result of acarbose molecule desorption from the surface of low-carbon steel **[**11].

The potential for corrosion varies slightly with the EBHL concentration and does not change the appearance of anodic and cathodic branches, confirming the mixed nature of this extract **[**12, 13**]**. The Table 4 shows that the decrease in the corrosion current density is due to the inhibitory effect of the extract components, which are retained on the outer layer of the metal. This effectively blocks its active sites **[**13**]**, with a maximum efficiency of about 80% at 700 mg/L.

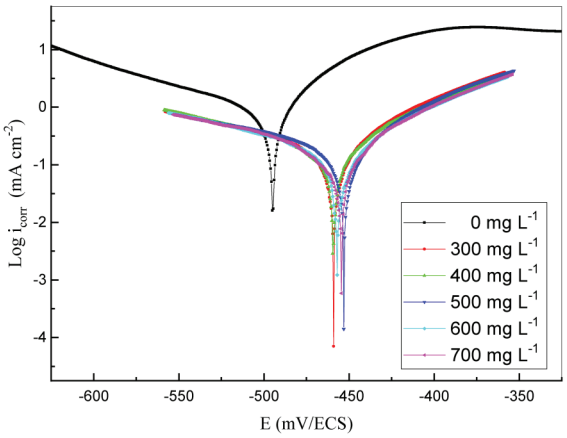

Fig 4. Polarization curves of API 5LGr-B metal in 1 M HCl solution and varying level of EBHL

3. 3. 3. Electrochemical Analysis of Impedance

Figure 5 displays the impedance diagrams according to the Nyquist description at a temperature of 298 K with and without the use of EBHL. According to the Nyquist diagrams, it was noted that with an increase in the concentration of the inhibitor after its introduction, the diameters of the capacitive semicircles increase. These graphs can represent a continuous capacitive ring, with a greater or lesser degree of flattening. Such a loop typically signifies a charge transfer process occurring on a solid electrode, where the corrosion reaction is regulated by an uneven and non-uniform surface structure **[**7**]**. The addition of EBHL reduces the value of the C_{dc} double layer forming capability and increases the load transfer resistance value. The decrease in the C_{dc} value may be due to adsorption of inhibitor molecules, which form a protective coating on the outer layer of

Table 4. Recovery rates, electrolytic factors and the efficiency of deteriorative inhibition of API 5LGr-B steel in 1M HCl solution without and with varying concentrations of EBHL at 293 K.

C (mg· L^{-1})	**EBHL**η					
	$-E_{corr}$ (mV)	i_{corr} (mA.cm^{-2})	β_a (mV.dec^{-1})	$-\beta_c$ (mV.dec^{-1})	Θ	η_p (%)
0	494.4	0.7921	45.3	119.7	-	-
300	459	0.3095	88.5	167.9	0.6094	60.92
400	459.1	0.2292	81.4	165.6	0.7107	71.04
500	452.8	0.2049	67	178.4	0.7414	74.13
600	457	0.1948	77.7	161.3	0.7541	75.41
700	454.7	0.1566	64.6	142.5	0.8023	80.23

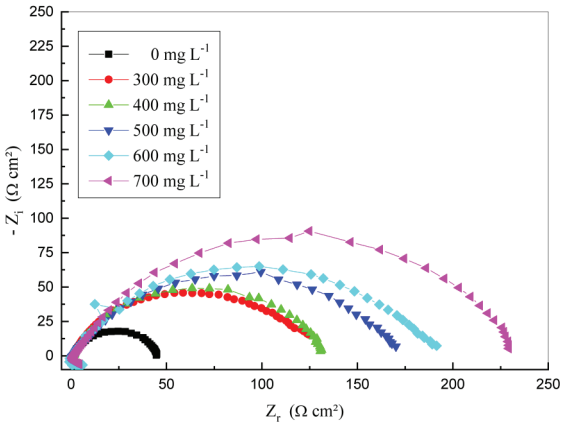

Fig 5. Electrochemical impedance of API 5LGr-B steel in 1 M HCl solution with several levels of EBHL (illustration in Nyquist plane)

API 5L Gr-B steel [14]. At the electrode-solution interface, the bilayer structure acts as an electrical capacitor, with its capacitance decreasing as water molecules in the electrolyte are displaced by adsorbed inhibitor molecules on the API 5L Gr-B metal outer surface. This process creates a protective layer, thereby lowering the number of active corrosion sites **[**15**]**.

Table 5 lists the impedance parameters when the lower C_{dc} values are contrasted with acid. This may be due to the formation of a protective layer on the outer surfaces of the mild iron, which inhibits corrosion. The addition of EBHL decreases the value of the capacity C_{dc} of the double layer and elevates the load transfer resistance. The decrease in the C_{dc} value can be explained by the retention of inhibitor components on the API 5L Gr-B metallic surface, causing the formation of a protective layer **[**14**]**. The double layer at the electrode-solution interface, considered as an electric capacitor, experiences a decrease in capacitance due to the replacement of water molecules in the electrolyte by inhibitor molecules adsorbed on the surface of the API 5L Gr-B metal. This results in the formation of a protective layer that minimizes the active corrosion sites **[**15**]**. The charge transfer resistance rises as the concentration of EBHL increases. This can be explained by the enhancement of the protective properties of the inhibiting oxide layer, which leads to an increase in R_{tc} values.

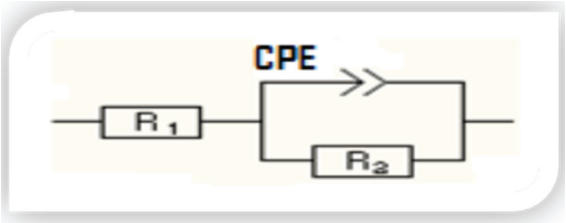

Fig. 6. EEC of API 5LGr-B steel in 1M HCl Solution containing and not containing EBHL.

3.3.4. Electric Equivalent Circuit (EEC)

The circuit developed for simulation studies within the EC-Lab program is shown in Figure 6. In the impedance range at high frequencies, a unique capacitive loop is observed whose diameter increases with increasing concentration, as shown by Nyquist plots. This means that the deterioration process is controlled by the combined effect of the charge transfer mechanism and the retention of EBHL on the metal surface, which leads to the formation of a protective, inhibitory film **[**7, 16**]**. Such loops are not ideal semicircles and may be due to the heterogeneity and roughness of the CS surfaces **[**17**]**. In cases where the virtual circuit curve is similar to our experimental curve (Figure 7), the solution resistance (R_1), bias resistance ($R_2 = R_{tc}$), and a constant phase factor (CPE) are present in this circuit. This circuit is

Table 5. Electrochemical parameters of the electrochemical impedance spectroscopy of API 5L Gr-B metal in HCl 1 M.

C (mg·L^{-1})	EBHL			
	R_{tc} (Ω·cm²)	C_{dc} (μF·cm^{-2})	θ	*EI*(%)
0	45.92	365	-	-
300	127.4	138	0.6396	63.96
400	135.7	120	0.6736	67.36
500	180.7	87	0.7549	75.49
600	201.1	80	0.7798	77.98
700	239.7	69	0.8152	81.52

Table 6. Kinetic parameters, recovery rates, and inhibition efficiency of steel in 1M HCl at different temperatures, in mixtures containing and not containing 700 mg/L EBHL additive.

T (°C)	EBHL						
	C mg L^{-1}	$-E_{corr}$ (mV)	i_{corr} (mA cm^{-2})	β_a (mV dec^{-1})	$-\beta_c$ (mV dec^{-1})	θ	*EI* (%)
20	0	494.4	0.7921	45.3	119.7	-	-
	700	454.7	0.1566	64.6	142.5	0.8023	80.23
30	0	483.8	0.7951	122.9	148.9	-	-
	700	462.2	0.1683	80.5	131.8	0.7883	78.83
40	0	506.5	1.8721	198.1	211.8	-	-
	700	395.4	0.6878	60.9	121.4	0.6326	63.26
50	0	504.2	2.2930	177.3	186.2	-	-
	700	484.7	0.9711	137.1	132.3	0.5765	57.65

Table 7. Electrochemical impedance test re sults in 1M HCl at various degrees, both with and without the addition of 700 mg L^{-1} of EBHL.

T (°C)	EBHL				
	C mg L^{-1}	R_{tc} (Ω·cm²)	C_{dc} (μF cm^{-2})	θ	*EI* (%)
20	0	45.92	365	-	-
	700	239.7	69	0.8152	80.84
30	0	40.39	380	-	-
	700	173.2	90	0.7668	76.68
40	0	32.78	412	-	-
	700	89.86	150	0.6323	63.23
50	0	23.37	502	-	-
	700	55.15	210	0.5762	57.62

in a good agreement with the electrochemical impedance measurements.

3.3.5. The impact of temperature

The results obtained from the corrosion temperature study of API 5L Gr-B metal in 1 M HCl with and without EBHL in the 293-323 K temperature range revealed that increasing temperature results in an increase in the corrosion rate and a decrease in inhibition efficiency for all concentrations.

3.4. Surface chemistry and morphological investigations

Figure 10 shows a scanning electron microscope image of the surface of low-carbon steel and EBHL inhibitor in an acidic environment. In the absence of the inhibitor, the specimen exhibits a highly rough surface, likely caused by the degradation of the rubber. In contrast, the SEM image of the mild steel sample in the inhibiting solution shows a significantly smoother surface [18]. It suggests that a highly effective protective layer has been deposited on the metal surface, leading to improved corrosion inhibition. Roughness values were determined for the ground metal under three different conditions: the steel sample in a control solution and the steel sample in an inhibited solution. Figure 10 shows that the steel cups in the inhibited solution exhibit significantly lower roughness compared to the mild steel sample in the uninhibited solution [19]. This is a stronger inhibitory effect that activates a protective shield on the outer layer of low carbon steel and prevents the solution from penetrating and destroying the steel [20].

3.5. X-ray Photoelectron Spectrometry (XPS)

Figure 11 shows the XPS overview spectra of the films before and after SUB treatment. As expected, the surfaces of all samples contain carbon (C), iron (Fe), and oxygen (O).

Figure 12 shows the higher resolution deconvoluted XPS spectra of the C 1s sample with

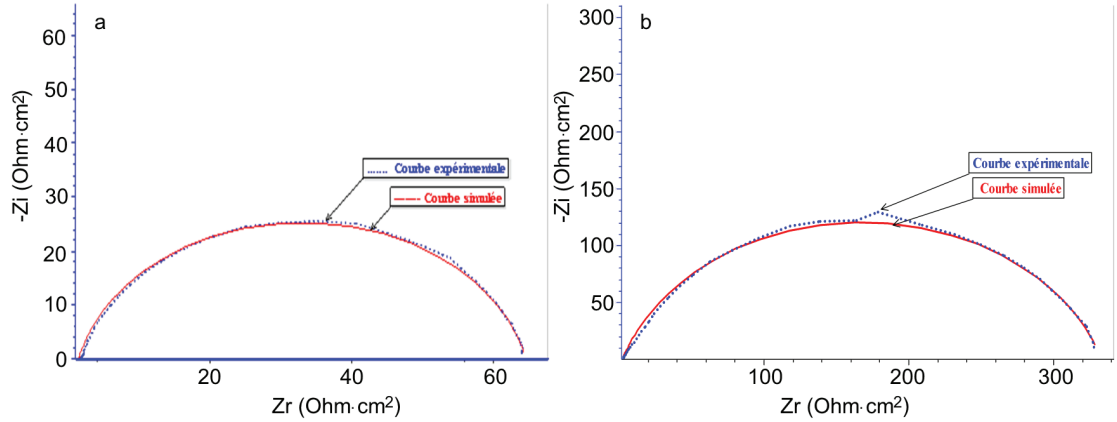

Fig. 7. Experimental and simulated steel impedance curves API 5L Gr-B in 1 M HCl. a – without the addition of EBHL; b – with the addition of 700 mg L^{-1} EBHL

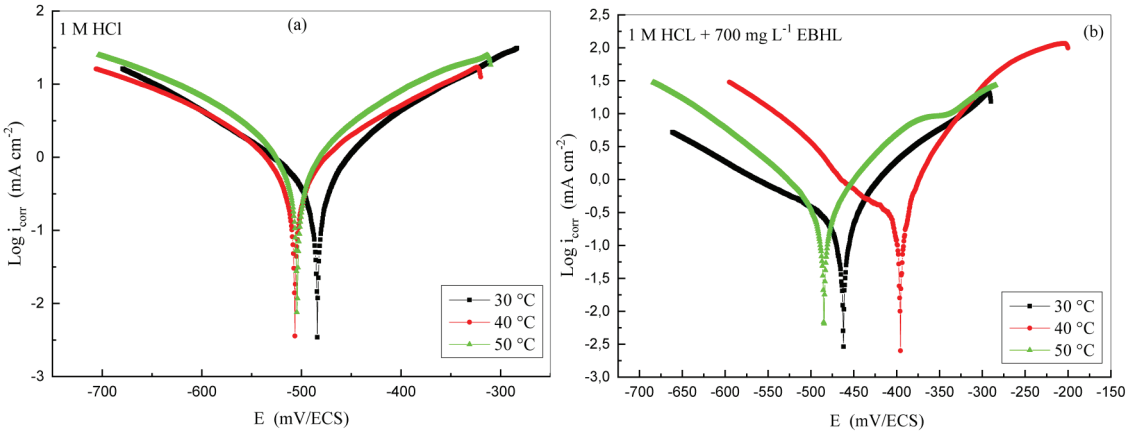

Fig. 8. Polarization curves obtained at temperatures of (30, 40 and 50) °C in 1 M HCl solution: (a) without EBHL, (b) with 700 mg/L EBHL.

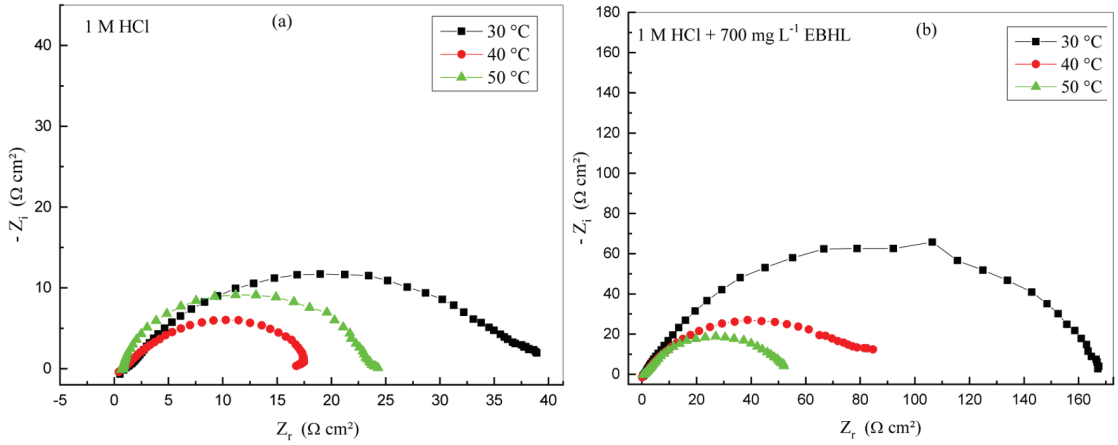

Fig. 9. S.I.E. curves obtained for temperatures (30, 40 and 50) °C in the 1 M HCl solution: (a) without adding EBHL, (b) with the addition EBHL of 700 mg L^{-1}

and without SUB. The peaks at 290, 284.4, 288.1 and 286.1 correspond to (COOH), (C O), C-H and C-C bonds on the carbide phase surface.

Fig. 16 shows the XPS study spectra before and after the SUB treatment. Iron (Fe^{2+}), (Fe^{3+}) and (Fe^{+1}) are present on the surfaces of all samples.

3. Conclusion

The aim of this work was to evaluate the Hippomarathrum libanotis plant as a corrosion inhibitor. Electrochemical impedance spectroscopy (EIS) and potentiodynamic polarization are used to study the anticorrosion effect of the

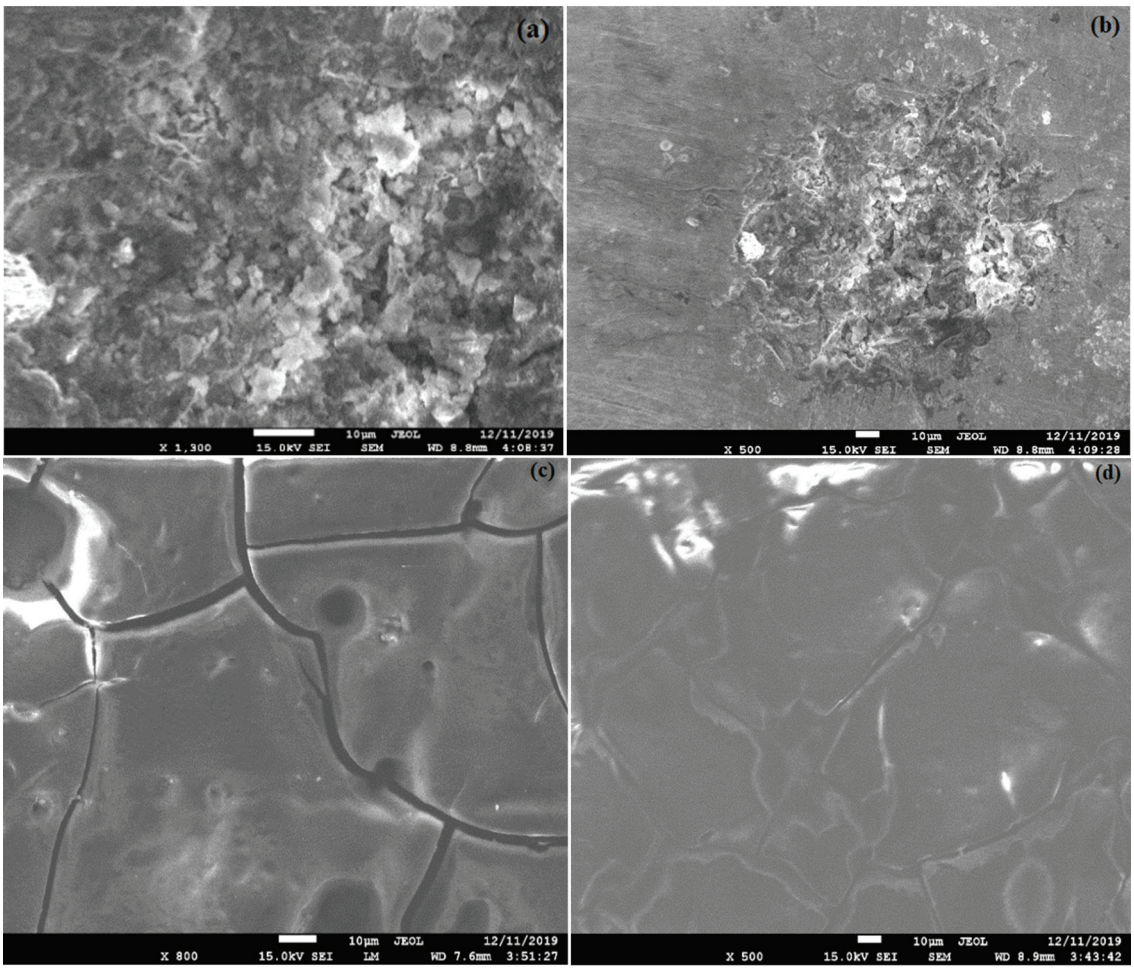

Fig. 10. SEM of a steel immersed in an HCl solution without inhibitor (a), (b); pictures of a mild steel immersed in an inhibited solution (c), (d).

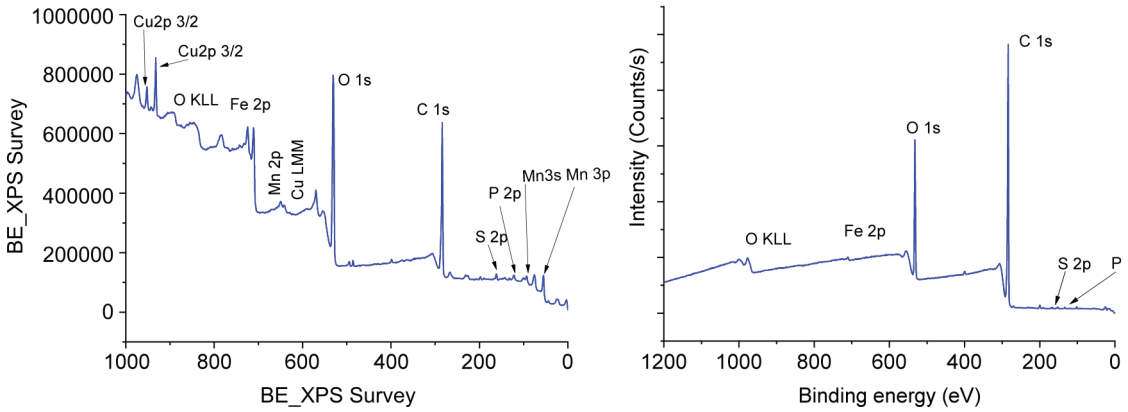

Fig. 11. XPS overview spectra without and with EBHL.

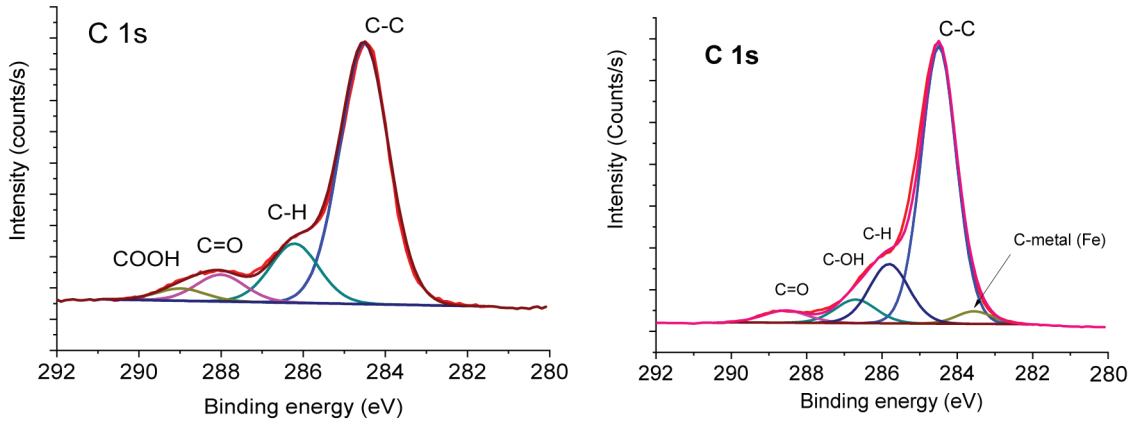

Fig. 12. XPS C1s higher resolution spectra of samples without and with EBHL.

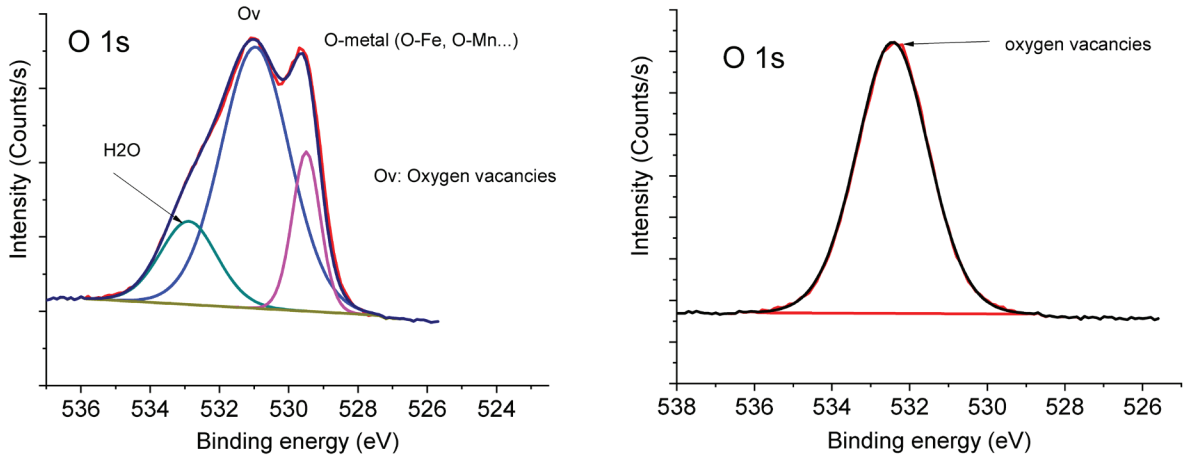

Fig. 13. XPS O1s higher resolution spectra of sample without and with EBHL.

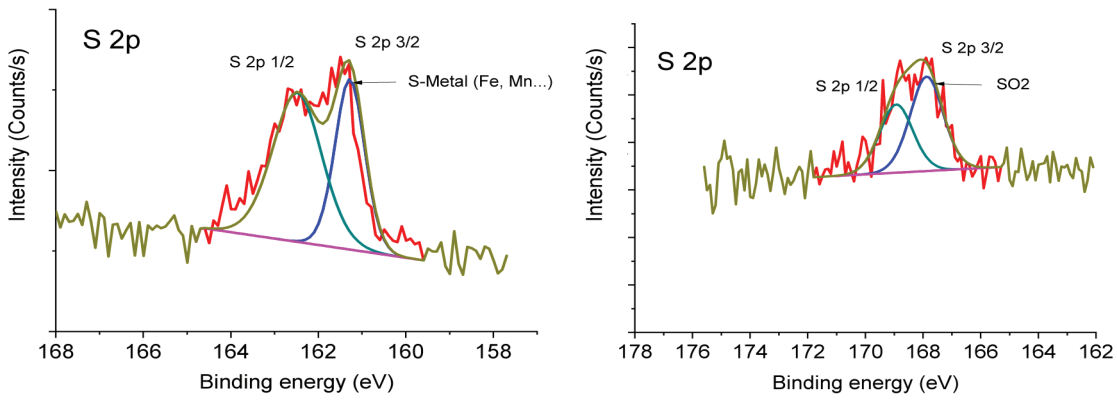

Fig. 14. XPS S 2p higher resolution spectra of sample without and with EBHL.

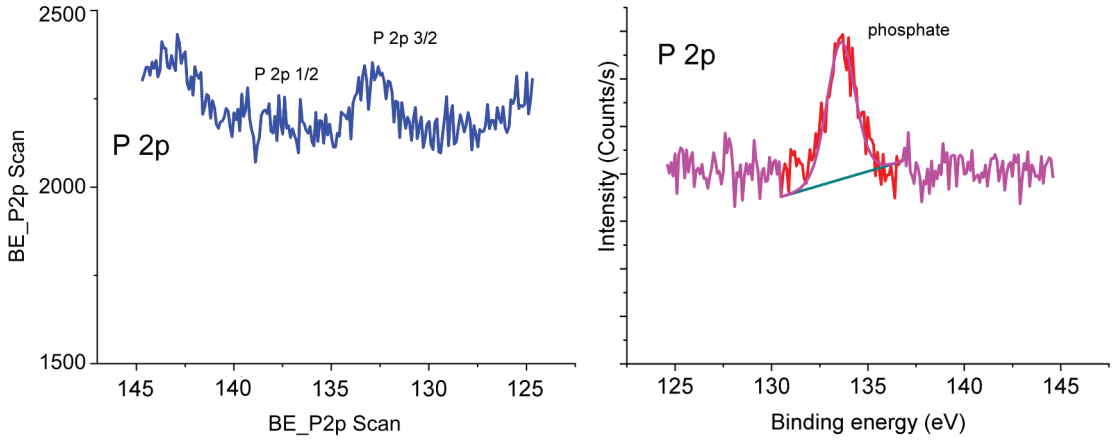

Fig. 15. XPS P 2p higher resolution spectra of sample without and with EBHL.

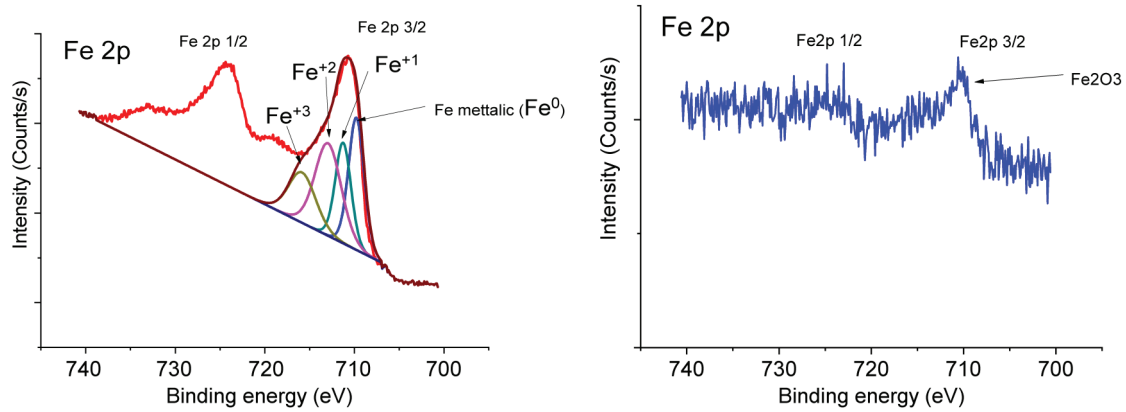

Fig. 16. XPS Fe 2p higher resolution spectra of sample without and with EBHL

butanol extract of Hippomararthum libanotis. Polarization curves show that the extract is an excellent mixed inhibitor. Maximum inhibition efficiency of 80.23% was achieved with 700 mg/L of the inhibitor at 298 k. This investigation is complemented by morphological and surface chemistry studies using scanning electron microscopy (SEM) respectively. The results confirm the formation of a protective layer on the surface of the extract.

References

1. V. L. Singleton, J. A. Rossi. Am. J. Enol. Vitic. 1965, 16, 144–158.
2. Bashir, Sumayah, et al. «Computational and experimental studies on Phenylephrine as anti-corrosion substance of mild steel in acidic medium.» Journal of Molecular Liquids 293 (2019): 111539.
3. Kumar, Ashish, and Sumayah Bashir. "Ethambutol: A new and effective corrosion inhibitor of mildsteel in acidic medium." Russian Journal of Applied Chemistry 89.7 (2016): 1158-1163.
4. El-Yaktini, A., et al. «Practical and Theoretical Study on the Inhibitory Influences of New Azomethine Derivatives Containing an 8-Hydroxyquinoline Moiety for the Corrosion of Carbon Steel in 1 M HCl.» Oriental Journal of Chemistry 34.6 (2018): 3016-3029.
5. Singh, Ambrish, et al. «Effect of electron donating functional groups on corrosion inhibition of mild steel in hydrochloric acid: Experimental and quantum chemical study.» Journal of the Taiwan Institute of Chemical Engineers 82 (2018): 233-251.
6. Wedian, Fadel, Mahmoud A. Al-Qudah, and Ghassab M. Al-Mazaideh.»Corrosion inhibition of copper by Capparisspinosa L. extract in strong acidic medium: experimental and density functional theory.» Int J Electrochem Sci 12 (2017): 4664-4676.
7. Anusuya, N., et al. «Corrosion inhibition effect of hydroxy pyrazoline derivatives on mildsteel in

sulphuricacid solution together with Quantum chemical studies.» J. Mater. Environ. Sci 6.6 (2015): 1606-1623.
8. Saha, Sourav Kr, et al. «Adsorption and corrosion inhibition effect of Schiff base molecules on the mild steel surface in 1 M HCl medium: a combined experimental and theoretical approach.» Physical Chemistry Chemical Physics 17.8 (2015): 5679-5690.
9. Lgaz, Hassane, et al. «Correlated experimental and theoretical study on inhibition behavior of novelquinoline derivatives for the corrosion of mildsteel in hydrochloricacid solution.» Journal of Molecular Liquids 244 (2017): 154-168.
10. Bashir, Sumayah, Garima Singh, and Ashish-Kumar. «An investigation on mitigation of corrosion of aluminium by Origanumvulgare in acidic medium.» Protection of Metals and Physical Chemistry of Surfaces 54.1 (2018): 148-152.
11. Solmaz, Ramazan. «Investigation of corrosion inhibition mechanism and stability of Vitamin B1 on mildsteelin 0.5 M HCl solution.» Corrosion Science 81 (2014): 75-84.
12. Bashir, Sumayah, et al. «Potential of Venlafaxine in the inhibition of mildsteel corrosion in HCl: insights from experimental and computational studies.» Chemical Papers 73.9 (2019): 2255-2264.
13. Keleş, Hülya, Duygu Melis Emir, and Mustafa Keleş. «A comparative study of the corrosion inhibition of lowcarbonsteel in HCl solution by an imine compound and its cobalt complex.» corrosion science 101 (2015): 19-31.
14. Anaee, R. A., W. M. Salih, and H. A. Abdullah. «Anodic Inhibitor Doped Polypyrrole Coating to Reduce Corrosion in Petroleum Medium.» Engineering and Technology Journal 35.9 Part (A) Engineering (2017): 878-886.
15. Verma, Chandrabhan, et al. «Adsorption behavior of glucosamine-based, pyrimidine-fusedheterocycles as green corrosion inhibitors for mildsteel: experimental and theoretical studies.» The Journal of Physical Chemistry C 120.21 (2016): 11598-11611.
16. Pavithra, M. K., et al. «Inhibition of mildsteel corrosion by Rabeprazolesulfide.» Corrosion Science 60 (2012): 104-111.
17. Bedair, M. A., et al. «Empirical and theoretical investigations on the corrosion inhibition characteristics of mildsteel by three new Schiff base derivatives.» Journal of Adhesion Science and Technology 33.11 (2019): 1139-1168.
18. Qiang, Yujie, et al. «Evaluation of Ginkgo leaf extract as an eco-friendly corrosion inhibitor of X70 steel in HCl solution.» Corrosion Science 133 (2018): 6-16.
19. Bashir, Sumayah, et al. «Electrochemical behavior and computational analysis of phenylephrine for corrosion inhibition of aluminum in acidic medium.» Metallurgical and Materials Transactions A 50.1 (2019): 468-479.
20. Singh, Ambrish, et al. «A combined electrochemical and theoretical analysis of environmentally benign polymer for corrosion protection of N80 steel in sweet corrosive environment.» Results in Physics 13 (2019): 102116.